Original Article

Comparison of initial high-resolution computed tomography (HRCT) features of coronavirus disease 2019 (COVID-19) pneumonia and other viral pneumonias

Yilong Huang[1#], Yuanming Jiang[1#], Zhenhui Li[2#], Dan Han[1], Li Wu[1], Jiyao Ma[1], Peng Wang[3], Ying Xie[4], Zhipeng Li[5], Xiang Li[6], Minchang Hong[7], Jialong Zhou[8], Chuwei Duan[9], Yunhui Yang[10], Wei Zhao[1], Feng Yuan[1], Kunhua Wang[11], Wenfang Yi[1], Bo He[1,11]

[1]Medical Imaging Department, First Affiliated Hospital of Kunming Medical University, Kunming, China; [2]Medical Imaging Department, Yunnan Cancer Hospital & The Third Affiliated Hospital of Kunming Medical University, Kunming, China; [3]Radiology Department, the Second People's Hospital of Yunnan Province, Kunming, China; [4]Department of Radiology, Calmette Hospital & The First Hospital of Kunming, Kunming, China; [5]Medical Imaging Department, Yunnan Provincial Infectious Disease Hospital (Yunnan AIDS Care Center), Kunming, China; [6]Department of Radiology, The 3rd People's Hospital of Kunming, Kunming, China; [7]Department of Radiology, the First People's Hospital of Zhaotong, Zhaotong, China; [8]MRI Department, The First People's Hospital of Yunnan Province, Kunming, China; [9]Radiology Department, Yan'an Hospital of Kunming, Kunming, China; [10]Department of Medical Imaging in People's Hospital of Xishuangbanna Dai Autonomous Prefecture, Jinghong, China; [11]NHC Key Laboratory of Drug Addiction Medicine, First Affiliated Hospital of Kunming Medical University, Kunming Medical University, Kunming, China

Contributions: (I) Conception and design: Y Huang, W Yi, B He; (II) Administrative support: D Han, K Wang, B He; (III) Provision of study materials or patients: P Wang, Y Xie, Z Li, X Li, M Hong, J Zhou, C Duan, Y Yang, W Zhao; (IV) Collection and assembly of data: Y Jiang, Z Li, L Wu, J Ma, F Yuan; (V) Data analysis and interpretation: Y Huang, Y Jiang, Z Li, L Wu, J Ma, B He; (VI) Manuscript writing: All authors; (VII) Final approval of manuscript: All authors.

[#]These authors contributed equally to this work.

Correspondence to: Bo He. NHC Key Laboratory of Drug Addiction Medicine, Medical Imaging Department, First Affiliated Hospital of Kunming Medical University, Kunming Medical University, Kunming, China. Email: hebo_ydyy@qq.com; Kunhua Wang. NHC Key Laboratory of Drug Addiction Medicine, First Affiliated Hospital of Kunming Medical University, Kunming Medical University, Kunming, China. Email: wangkunhua_ydyy@163.com; Wenfang Yi. Medical Imaging Department, First Affiliated Hospital of Kunming Medical University, Kunming, China. Email: 471991019@qq.com.

Background: Multicenter retrospective comparison of the first high-resolution computed tomography (HRCT) findings of coronavirus disease 2019 (COVID-19) and other viral pneumonias.

Methods: We retrospectively collected clinical and imaging data from 262 cases of confirmed viral pneumonia in 20 hospitals in Yunnan Province, China, from March 1, 2015 to March 15, 2020. According to the virus responsible for the pneumonia, the pneumonias were divided into non-COVID-19 (141 cases) and COVID-19 (121 cases). The non-COVID-19 pneumonias comprised cytomegalovirus (CMV) (31 cases), influenza A virus (82 cases), and influenza B virus (20 cases). The differences in the basic clinical characteristics, lesion distribution, location and imaging signs among the four viral pneumonias were analyzed and compared.

Results: Fever and cough were the most common clinical symptoms of the four viral pneumonias. Compared with the COVID-19 patients, the non-COVID-19 patients had higher proportions of fatigue, sore throat, expectorant and chest tightness (all $P<0.000$). In addition, in the CMV pneumonia patients, the proportions of acquired immunodeficiency syndrome (AIDS) and leukopenia were high (all $P<0.000$). Comparison of the imaging findings of the four viral pneumonias showed that the pulmonary lesions of COVID-19 were more likely to occur in the peripheral and lower lobes of both lungs, whereas those of CMV pneumonia were diffusely distributed. Compared with the non-COVID-19 pneumonias, COVID-19 pneumonia was more likely to present as ground-glass opacity, intralobular interstitial thickening, vascular thickening and halo sign (all $P<0.05$). In addition, in the early stage of COVID-19, extensive consolidation, fibrous stripes, subpleural lines, crazy-paving pattern, tree-in-bud, mediastinal lymphadenectasis, pleural

thickening and pleural effusion were rare (all P<0.05).

Conclusions: The HRCT findings of COVID-19 pneumonia and other viral pneumonias overlapped significantly, but many important differential imaging features could still be observed.

Keywords: Computed tomography; coronavirus disease 2019; viral pneumonia; X-ray computed tomography

Submitted Nov 19, 2020. Accepted for publication Jan 17, 2021.
doi: 10.21037/apm-20-2479
View this article at: http://dx.doi.org/10.21037/apm-20-2479

Introduction

Coronavirus disease 2019 (COVID-19) is highly infectious, has a long incubation period and is caused by severe acute respiratory syndrome coronavirus 2 (SARS-CoV-2) (1,2). COVID-19 spreads at an alarming rate. As of April 20, COVID-19 had spread to 211 countries worldwide, with more than 2.3 million confirmed patients and 164,976 deaths. Currently, COVID-19 has become a global health crisis.

Early studies showed that almost all COVID-19 patients have pneumonia (3,4). However, at the same time of year, pneumonias caused by other pathogens are also common (5-7). Therefore, in this COVID-19 pandemic, the differential diagnosis of viral pneumonias is difficult but very important. Real-time quantitative reverse transcription-polymerase chain reaction (qRT-PCR) is the gold standard for the diagnosis of viral pneumonia. However, recent reports have shown that the sensitivity of qRT-PCR for the detection of COVID-19 is as low as 60–71% (8), and the high false-negative rate limits the rapid identification of viral pneumonia by qRT-PCR.

Computed tomography (CT) can play an important role in the diagnosis and treatment of viral pneumonia (9-11). Studies have shown that the typical CT findings of COVID-19 include ground-glass opacity (GGO) and partial consolidation in the peripheral areas of both lungs with a round shape and without cavities, pleural effusion and lymphadenopathy (12,13). After treatment, chest CT can detect the dynamic changes in COVID-19 (14,15). Other studies have shown that the imaging findings of viral pneumonias and bacterial pneumonias are different (9,10), but little is known about the differences in imaging findings between COVID-19 and other viral pneumonias.

Therefore, the purpose of this study was to clarify the basic clinical features and potential differences in high-resolution computed tomography (HRCT) findings of COVID-19 and other viral pneumonias.

We present the following article in accordance with the STROBE reporting checklist (available at http://dx.doi.org/10.21037/apm-20-2479).

Methods

Patients

The study was conducted in accordance with the Declaration of Helsinki (as revised in 2013). The retrospective study was approved by the institutional committee of the First Affiliated Hospital of Kunming Medical University. Informed consent was waived because the study was retrospective in design. This multicenter study retrospectively analyzed patients who underwent chest CT for suspected viral pneumonia because of fever, fatigue or respiratory tract symptoms at 20 hospitals in Yunnan Province, China, from March 1, 2015, to March 15, 2020. qRT-PCR assays were performed to identify influenza A virus, influenza B virus, respiratory syncytial virus, parainfluenza virus, adenovirus, SARS coronavirus, SARS-CoV-2, Epstein-Barr virus, measles virus, and other viruses from nasopharyngeal swabs or bronchoalveolar lavage fluid. The study only included pneumonia patients infected with one virus, and patients with multiple respiratory viruses or bacterial or fungal infections were excluded (10 cases, 2.83%). A total of 353 viral pneumonia patients were included in this study. The selection process for viral pneumonia patients is shown in *Figure 1*. According to the clinical guidelines for COVID-19 (16), of 121 COVID-19 patients, 22 were mild, 76 were moderate, 20 were severe, and 3 were critical. In addition, the study excluded one case of Epstein-Barr virus, two cases of herpes virus, one case of measles virus, two cases of varicella virus, one case of mumps virus and one case of adenovirus. All patients were admitted within 4–7 days after the onset of acute symptoms. The patient's age, sex, history of exposure, and clinical symptoms (fever, cough, fatigue, dyspnea, sore throat, runny nose, expectoration, headache, muscle aches, chest tightness, chest pain, nausea and vomiting,

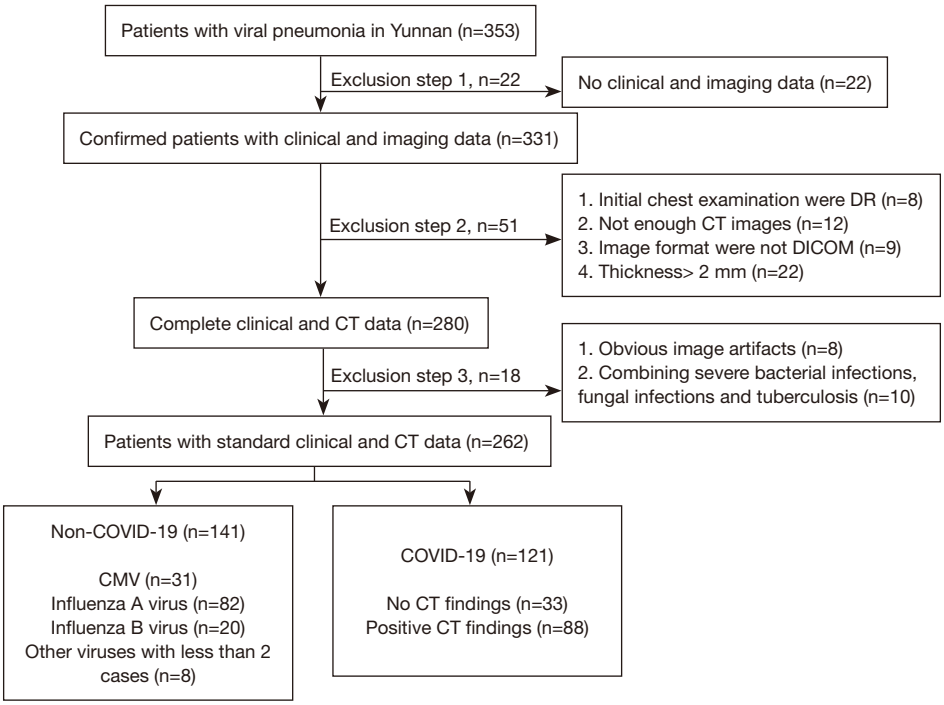

Figure 1 Flowchart of the study design and the participants included in the analysis. COVID-19, coronavirus disease 2019; CMV, cytomegalovirus; CT, computed tomography. DR, digital radiography; DICOM, digital imaging and communications in medicine.

diarrhea or no obvious symptoms), underlying diseases [hypertension, diabetes, coronary heart disease, liver disease, tumor, acquired immunodeficiency syndrome (AIDS) and leukopenia], hospital admission time and CT examination time were recorded. Patients completed the chest CT examination within 48 h of admission. According to the virus found in the lungs, the patients were divided into four groups: cytomegalovirus (CMV), influenza A virus, influenza B virus and COVID-19. The number of cases from each hospital is shown in *Table 1*. All patients were from Yunnan Province, China.

CT protocol

HRCT examination: CT scanners with ≥16 detector rows (Siemens, Germany; Philips, The Netherlands; and GE, USA) were used. The patient was scanned in the supine position while breath holding after inhalation. The scanning range was from the thoracic inlet to the costophrenic angles. Scanning parameters: detector collimation width 64 mm × 0.6 mm or 128 mm × 0.6 mm, tube voltage 120 kV, adaptive tube current, high-resolution algorithm reconstruction, reconstruction layer thickness 1 or 1.5 mm and layer spacing 1.5 mm. CT machines dedicated to COVID-19 patients are used for chest examinations, using disposable sheets to avoid cross-infection. After the patient's CT examination, disinfect the examination bed and floor, and disinfect the computer room and air with ultraviolet rays.

Chest CT analysis

Three radiologists were blinded to the qRT-PCR results, all patient information, and the type of viral pneumonia. First, two experienced radiologists (Yilong Huang and Yuanming Jiang) in the cardiothoracic group independently read the radiographs. When their opinions were inconsistent, they discussed them and reached a consensus, which was reviewed and confirmed by the third senior radiologist in the cardiothoracic group (Bo He). The morphological signs of the first CT examination after admission were analyzed. The CT imaging evaluation included lesion distribution (peripheral, central), location (left upper lobe, left lower lobe, right upper lobe, right middle lobe and right lower lobe) and signs (GGO, partial consolidation, multifocal consolidation, focal consolidation, fibrous stripes, septal thickening, intralobular interstitial thickening, subpleural

Table 1 Institution and number of cases in this multicenter study

Institution	Total No. of cases	CMV	Influenza A virus	Influenza B virus	COVID-19
Kunming Third People's Hospital	71	2	31	5	30
Yunnan Provincial Infectious Disease Hospital	50	27	8	0	12
Kunming First People's Hospital	30	0	18	11	0
The First People's Hospital of Zhaotong	22	0	4	1	17
Third People's Hospital of Yunnan Province	15	1	12	2	0
Xishuangbanna People's Hospital	13	0	3	1	9
Qujing First People's Hospital	12	0	0	0	12
Dali People's Hospital	11	0	0	0	11
Yuxi People's Hospital	10	0	0	0	10
Lijiang People's Hospital	6	0	0	0	6
Second People's Hospital of Yunnan Province	5	1	4	0	0
Chuxiong People's Hospital	4	0	0	0	4
Lancang First People's Hospital	3	0	0	0	3
First People's Hospital of Yunnan Province	2	0	2	0	0
Baoshan People's Hospital	2	0	0	0	2
Honghe People's Hospital	2	0	0	0	2
Pu'er People's Hospital	1	0	0	0	1
Qiaojia People's Hospital	1	0	0	0	1
Ruili People's Hospital	1	0	0	0	1
Total	262	31	82	20	121

Data are number of patients. CMV, cytomegalovirus; COVID-19, coronavirus disease 2019.

lines, crazy-paving pattern, tree-in-bud, bronchial wall thickening, bronchiectasis, vascular thickening, air bronchogram, halo sign, mediastinal lymphadenectasis, pleural thickening and pleural effusion) (9,10,12,17). The window width and level were set to 1,600/–600 Hounsfield units, respectively.

Statistical analysis

SPSS 25.0 software was used for statistical analysis. Count data are expressed as frequency, and measurement data are expressed as $\bar{x}\pm s$. One-way analysis of variance (ANOVA) was used for age, which had a normal distribution, and the least significant difference method was used for pairwise comparison. The distribution, location and signs of pulmonary lesions in different viral pneumonias were compared using χ^2 or Fisher's exact probability method. The Z-test (Bonferroni method) was used for pairwise comparisons. A P value <0.05 was considered statistically significant.

Results

Patients' clinical characteristics

This study included 262 patients with viral pneumonia, comprising 121 COVID-19 patients and 141 patients with non-COVID-19 pneumonias (CMV, 31 cases; influenza A virus, 82 cases, influenza B virus, 20 cases; other viruses with less than 2 cases, 8). The mean age of the COVID-19 patients (42.88±17.67) was lower than that of the influenza A patients (55.50±18.46). Of the 121 COVID-19 patients, 54 (44.63%) were male, and 97 (68.79%) of the 141 non-COVID-19 patients were male. All COVID-19 patients had a history of living in Hubei or had close contact with

other COVID-19 patients. Five patients with influenza A had a history of poultry contact. Among the four viral pneumonias, fever and cough were the most common clinical symptoms, and the highest proportion was found in the influenza A patients (P<0.000). Compared with the COVID-19 patients, the non-COVID-19 patients had higher proportions of fatigue, sore throat, expectoration and chest tightness, whereas the COVID-19 patients were more likely to be asymptomatic, and the differences were statistically significant (all P<0.000). Compared with the other viral pneumonia patients, the CMV pneumonia patients had higher proportions of AIDS and leukopenia (all P<0.000). *Table 2* shows the clinical characteristics of the included patients.

Distribution and location of the pulmonary lesions of COVID-19 and other viral pneumonias

On the first CT examination, 33 COVID-19 patients were negative. *Figure 2* shows the comparisons of the distribution and location of pulmonary lesions found on the first CT examinations of CMV, influenza A virus, influenza B virus, non-COVID-19 and COVID-19 patients. There were no lesions in the central lung alone in the COVID-19 patients. The proportion of peripheral lesions in the COVID-19 patients was significantly higher than in the patients with other viral pneumonias (all P<0.000), and the pulmonary lesions of CMV pneumonia were mainly distributed in the peripheral and central lung. Regarding the pulmonary lesions in COVID-19, influenza A virus and influenza B virus, more were found in the left and right lower lobes than in other lung lobes (P<0.05). However, in the CMV pneumonia patients, there was no significant difference in the number of lesions found in the different lung lobes; however, more CMV patients than patients with other viral pneumonias had lesions in the left upper lobe, right upper lobe, and right middle lobe, and the differences were statistically significant (P<0.05).

Chest CT findings of viral pneumonia

The first CT images of pulmonary lesions in CMV, influenza A virus, influenza B virus, Non-COVID-19 and COVID-19 were compared (*Table 3*). Compared with Non-COVID-19 pneumonias, COVID-19 was more likely to present as GGO (96.59% *vs.* 46.81%, P<0.001), intralobular interstitial thickening (63.64% *vs.* 19.15%, P<0.001), vascular thickening (55.68% *vs.* 4.96%, P<0.001) and halo signs (59.09% *vs.* 14.89%, P<0.001). In the early stage of COVID-19, extensive consolidation (7.95% *vs.* 39.72%, P<0.001), fibrous stripes (15.91% *vs.* 34.75%, P=0.001), subpleural lines (7.95% *vs.* 39.72%, P<0.001), crazy-paving pattern (0.00% *vs.* 14.18%, P<0.001), tree-in-bud (1.14% *vs.* 27.66%, P<0.001), mediastinal lymphadenectasis (14.18% *vs.* 1.14%, P<0.001), pleural thickening (56.74% *vs.* 38.64%, P=0.013) and pleural effusion (25.53% *vs.* 0.00%, P<0.001) were rare. *Table 4* shows the sensitivity, specificity, and accuracy of these meaningful signs in distinguishing COVID-19 from non-COVID-19. *Figures 3-6* show representative cases of CMV, Influenza A virus, Influenza B virus, and COVID-19 pneumonia.

Discussion

COVID-19 is threatening human health and safety worldwide. Considering the similarity in outbreak time and clinical manifestations between COVID-19 and other viral pneumonias, this study systematically analyzed the differences in the first chest CT findings between COVID-19 and other viral pneumonias. We found that although it is difficult to completely differentiate COVID-19 from other viral pneumonias, COVID-19 has some unique CT features.

We included 262 patients with confirmed viral pneumonia. The main clinical manifestations of all patients were fever and cough. However, the incidence of fever and cough in COVID-19 patients was low, which was consistent with previous results from Zhao *et al.* (18) and Tang *et al.* (19) and may be related to the low virulence of SARS-CoV-2. In this study, 15 patients (12.40%) showed no obvious clinical symptoms, and 33 patients (27.27%) had negative CT findings, which was consistent with the results of Guan *et al.* (2). However, the patients' RT-PCT results were still positive for SARS-CoV-2, indicating that they were still infectious and should be isolated for observation and antiviral treatment. It is worth noting that patients with AIDS or leukopenia were more prone to developing CMV pneumonia.

The periphery of the lower lobes of both lungs was the most common area for lesions in COVID-19 and influenza pneumonias, which is consistent with the results of previous studies (17). However, we found that a high proportion of COVID-19 lesions occurred in the peripheral area, whereas CMV pneumonia was usually diffusely distributed in both lungs. This study systematically analyzed and compared the CT findings of COVID-19 and other viral pneumonias. We found that GGO was more common in COVID-19 than in

Table 2 Basic clinical characteristics of 262 patients with viral pneumonia

Clinical characteristics	CMV (n=31)	Influenza A virus (n=82)	Influenza B virus (n=20)	Non-COVID-19 (n=141)	COVID-19 (n=121)	P value
Age (av.), years	41.55±10.69	55.50±18.46*	40.85±18.75	48.50±19.47*	42.88±17.67	0.000
Age range	28–76	6–93	6–72	0.5–93	3–79	
Sex, n (%)						0.000
Male	26 (83.87)*	56 (68.29)*	11 (55.00)	97 (68.79)*	54 (44.63)	
Female	5 (16.13)*	26 (31.71)*	9 (45.00)	44 (31.21)*	67 (55.37)	
Epidemiological history, n (%)						
Travel/residence history in Hubei	0 (0.00)	0 (0.00)	0 (0.00)	0 (0.00)	98 (80.99)	
Close contact with patients	0 (0.00)	16 (19.51)	2 (10.00)	19 (13.48)	23 (19.01)	
Exposure to infected poultry	0 (0.00)	5 (6.10)	0 (0.00)	5 (3.55)	0 (0.00)	
Symptoms, n (%)						
Fever	22 (70.97)	72 (87.80)*	16 (80.00)	118 (83.69)*	60 (49.59)	0.000
Cough	20 (64.52)	75 (91.46)*	8 (40.00)	103 (73.05)*	53 (43.80)	0.000
Fatigue	12 (38.71)*	32 (39.02)*	5 (25.00)	49 (34.75)*	17 (14.05)	0.000
Difficulty breathing	3 (9.68)	6 (7.32)	1 (5.00)	11 (7.80)	3 (2.48)	0.349
Sore throat	0 (0.00)	23 (28.05)*	2 (10.00)*	25 (17.73)	12 (9.92)	0.001
Runny nose	4 (12.90)	11 (13.41)	1 (5.00)	16 (11.35)	8 (6.61)	0.450
Expectorant	10 (32.26)*	32 (39.02)	8 (40.00)*	50 (35.46)*	18 (14.88)	0.001
Headache	1 (3.23)	4 (4.88)	1 (5.00)	6 (4.26)	7 (5.79)	0.972
Muscle ache	0 (0.00)	6 (7.32)	1 (5.00)	7 (4.96)	9 (7.44)	0.551
Chest tightness	21 (67.74)*	4 (4.88)	7 (35.00)	32 (22.70)*	9 (7.44)	0.000
Chest pain	0 (0.00)	2 (2.44)	1 (5.00)	3 (2.13)	3 (2.48)	0.838
Nausea and vomiting	0 (0.00)	0 (0.00)	0 (0.00)	0 (0.00)	2 (1.65)	0.336
Diarrhea	0 (0.00)	0 (0.00)	0 (0.00)	0 (0.00)	1 (0.83)	0.686
No obvious symptoms	0 (0.00)	0 (0.00)*	0 (0.00)	0 (0.00)*	15 (12.40)	0.000
Underlying disease, n (%)						
Hypertension	3 (9.68)	28 (34.15)*	10 (50.00)*	42 (29.79)*	9 (7.44)	0.000
Diabetes	2 (6.45)	19 (23.17)*	2 (10.00)	23 (16.31)*	7 (5.79)	0.004
Coronary heart disease	1 (3.23)	2 (2.44)	1 (5.00)	4 (2.84)	3 (2.48)	0.977
Liver disease	6 (19.35)	3 (3.66)	2 (10.00)	11 (7.80)	2 (1.65)	0.003
Malignant tumor	1 (3.23)	0 (0.00)	0 (0.00)	1 (0.71)	0 (0.00)	0.215
AIDS	22 (70.97)*	0 (0.00)	0 (0.00)	22 (15.60)*	0 (0.00)	0.000
Leukopenia	6 (19.35)*	0 (0.00)	0 (0.00)	6 (4.26)	0 (0.00)	0.000

Continuous data are expressed as mean ± SD, and categorical data are presented as n (%). *, compared with COVID-19, significance was considered when P<0.05. AIDS, acquired immune deficiency syndrome; CMV, cytomegalovirus; COVID-19, coronavirus disease 2019.

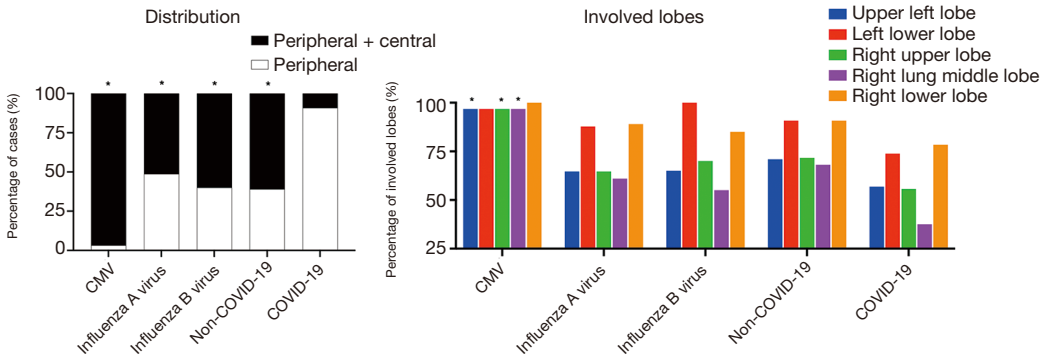

Figure 2 Distribution and location of COVID-19 pneumonia and other viral pneumonias: (A) lesion distribution and (B) lesion location. Data are reported as percentages. *, P<0.05 *vs.* COVID-19 pneumonia. COVID-19, coronavirus disease 2019; CMV, cytomegalovirus.

Table 3 Comparison of CT findings of different viral pneumonias

CT findings	CMV (n=31)	Influenza A virus (n=82)	Influenza B virus (n=20)	Non-COVID-19 (n=141)	COVID-19 (n=88)	P value
Main features						
GGO	8 (25.81)*	41 (50.00)*	12 (60.00)*	66 (46.81)*	85 (96.59)	0.000
Partial consolidation	22 (70.97)*	42 (51.22)	10 (50.00)	79 (56.03)	34 (38.64)	0.015
Consolidation						
Multifocal consolidation	14 (45.16)*	33 (40.24)*	6 (30.00)	56 (39.72)*	7 (7.95)	0.000
Focal consolidation	10 (32.26)	15 (18.29)	6 (30.00)	32 (22.70)	22 (25.00)	0.546
Fibrous stripes	6 (19.35)	30 (36.59)*	10 (50.00)*	49 (34.75)*	14 (15.91)	0.001
Interstitial changes						
Septal thickening	14 (45.16)	29 (35.37)	7 (35.00)	52 (36.88)	30 (34.09)	0.833
Intralobular interstitial thickening	7 (22.58)*	15 (18.29)*	5 (25.00)*	27 (19.15)*	56 (63.64)	0.000
Subpleural lines	3 (9.68)	27 (32.93)*	3 (15.00)	35 (24.82)*	7 (7.95)	0.000
Crazy-paving pattern	11 (35.48)*	7 (8.54)	2 (10.00)*	20 (14.18)*	0 (0.00)	0.000
Other features						
Tree-in-bud	2 (6.45)	28 (34.15)*	8 (40.00)*	39 (27.66)*	1 (1.14)	0.000
Bronchial wall thickening	6 (19.35)	17 (20.73)	2 (10.00)	26 (18.43)	12 (13.64)	0.618
Bronchiectasis	23 (74.19)*	19 (23.17)	6 (30.00)	49 (34.75)	23 (26.14)	0.000
Vascular thickening	2 (6.45)*	4 (4.88)*	1 (5.00)*	7 (4.96)*	49 (55.68)	0.000
Air bronchogram	14 (45.16)*	14 (17.07)	3 (15.00)	32 (22.69)	11 (12.50)	0.002
Halo sign	0 (0.00)*	12 (14.63)*	8 (40.00)	21 (14.89)*	52 (59.09)	0.000
Mediastinal lymphadenectasis	10 (32.26)*	9 (10.98)	0 (0.00)	20 (14.18)*	1 (1.14)	0.000
Pleural thickening	20 (64.52)	46 (56.10)	13 (65.00)	80 (56.74)*	34 (38.64)	0.013
Pleural effusion	7 (22.58)*	22 (26.83)*	5 (25.00)*	36 (25.53)*	0 (0.00)	0.000

Categorical data are presented as n (%). *, compared with COVID-19, significance was considered when P<0.05. CMV, cytomegalovirus; COVID-19, coronavirus disease 2019; GGO, ground-glass opacities.

Table 4 Diagnosis performance of CT findings in distinguishing COVID-19 from Non-COVID-19

CT findings	Sensitivity (%)	Specificity (%)	Accuracy (%)
GGO	96.59	53.19	69.87
Multifocal consolidation	7.95	60.28	40.17
Fibrous stripes	15.91	65.25	46.29
Intralobular interstitial thickening	63.64	80.85	74.24
Subpleural lines	7.95	75.18	49.34
Crazy-paving pattern	0.00	85.82	52.84
Tree-in-bud	1.14	72.34	44.98
Vascular thickening	67.05	95.04	84.28
Halo sign	59.09	85.11	75.11
Mediastinal lymphadenectasis	1.14	85.82	53.28
Pleural thickening	38.64	43.26	41.48
Pleural effusion	0.00	74.47	45.85

COVID-19, coronavirus disease 2019; GGO, ground-glass opacities.

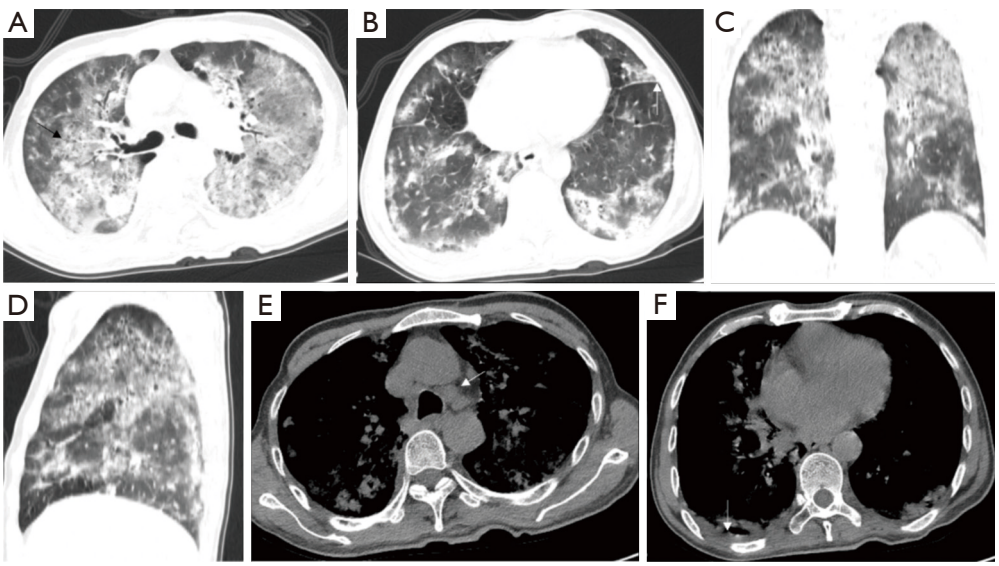

Figure 3 Chest CT findings in 54-year-old male with CMV pneumonia combined with AIDS and leukopenia. (A,B,C,D,E,F) Diffuse GGO and multifocal consolidation in both lungs. (A) Bronchiectasis (black arrow), (B) left intralobular interstitial thickening (white arrow), (E) mediastinal lymphadenectasis (white arrow), and (F) left pleural effusion (white arrow). (A,B,E,F): axial view; (C): coronal view; (D): sagittal view. AIDS, acquired immunodeficiency syndrome; COVID-19, coronavirus disease 2019; CMV, cytomegalovirus; CT, computed tomography; GGO, ground-glass opacity.

other viral pneumonias, and multifocal consolidation was more common in other viral pneumonias, a result that was consistent with previous studies (17,19). To the best of our knowledge, studies comparing the microscopic differences between COVID-19 and other viral pneumonias are still rare. The GGO, intralobular interstitial thickening, vascular thickening and halo sign were more likely to occur in COVID-19 than in other viral pneumonias, and fibrous

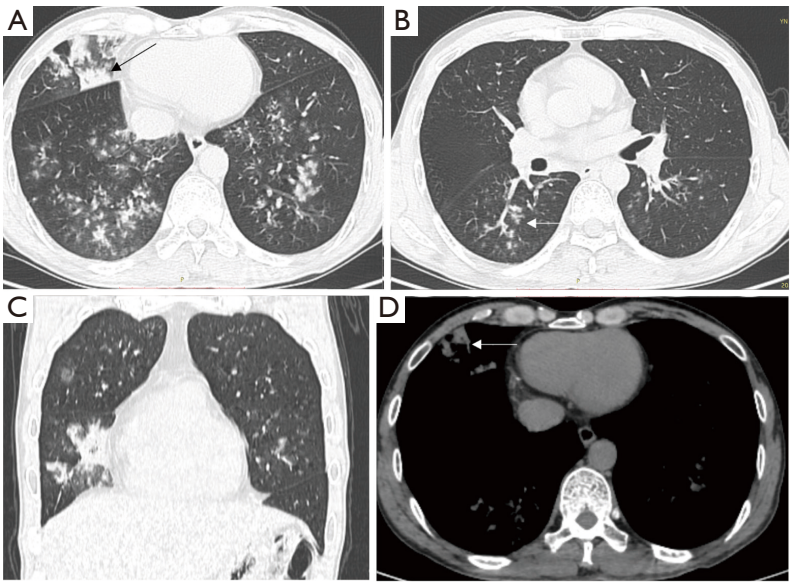

Figure 4 Chest CT findings of influenza A pneumonia in a 44-year-old male (H1N1 infection). (A,B,C,D) Multifocal GGO, partial consolidation and consolidation in both lungs (arrow in A, D shows consolidation in right middle lobe); (B) tree-in-bud (white arrow). (C) Coronal view. CT, computed tomography; GGO, ground-glass opacity.

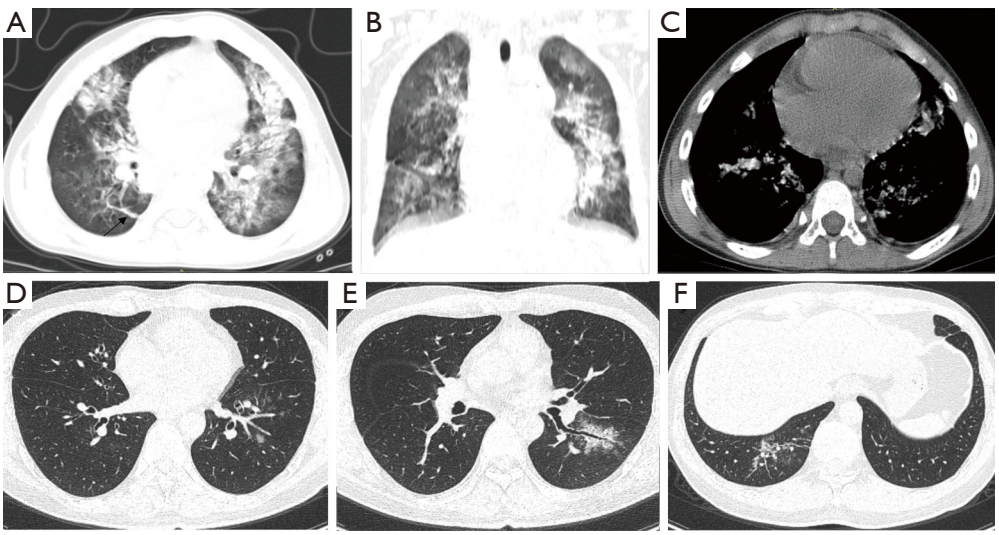

Figure 5 Chest CT findings of influenza B pneumonia in (A,B,C) 6-year-old male and (D,E,F) 39-year-old male. (A,B,C) Multifocal GGO with partial consolidation in both lungs with a parenchymal band (A, black arrow), air bronchogram, pleural thickening, and pleural effusion. (D) Multifocal GGO and tree-in-bud in lower lobes of both lungs, with bronchial wall thickening (E) and partial consolidation and parenchymal band (F). (A,B,C,D,E,F) Axial view.

stripes, subpleural lines, crazy-paving pattern, tree-in-bud, pleural effusion and mediastinal lymphadenectasis occurred less frequently in COVID-19 than in other viral pneumonias. The pathophysiological mechanisms of these characteristic imaging changes are still unclear. However, the difference in CT findings in COVID-19 and other viral pneumonia may be closely related to the difference in virus types. After autopsy of patients who died of COVID-19 and

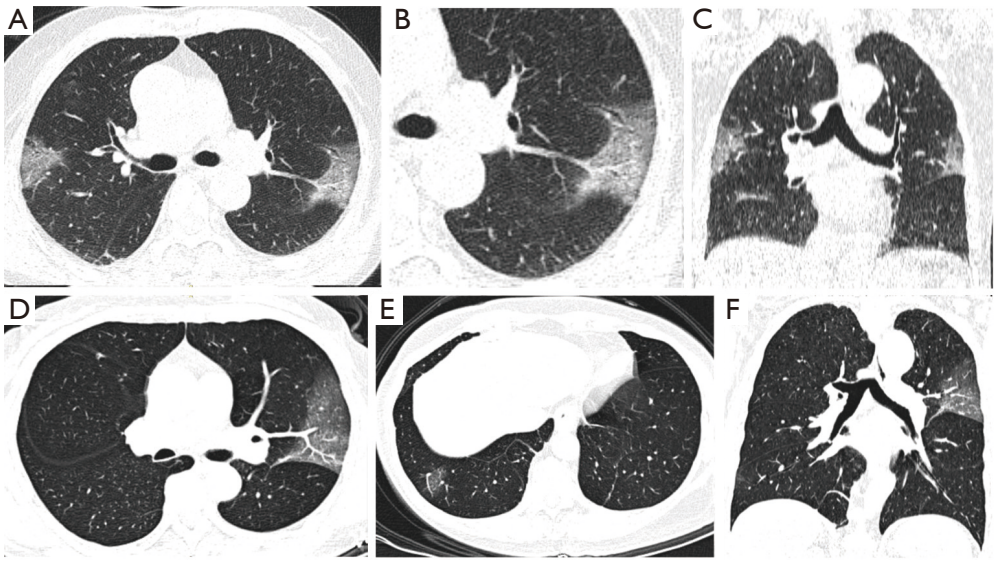

Figure 6 Chest CT findings of COVID-19 pneumonia in (A,B,C) 63-year-old female and (D,E,F) 66-year-old female. (A,B,C) Multifocal GGO in both lungs. (B) Vascular thickening and intralobular interstitial thickening, and (C) pleural thickening. (D,E,F) Multifocal GGO in both lungs. (D) Intralobular interstitial thickening, (D,E) vascular thickening and (F) pleural thickening. (A,B,D,F) Axial view; (C,F) coronal view.

influenza (20), histological results revealed diffuse alveolar injury with perivascular T cell infiltration in the peripheral lung tissue of COVID-19. The pulmonary vessels of Covid-19 patients have severe endothelial damage, and extensive thrombosis is accompanied by microvascular disease. The incidence of alveolar capillary thrombosis in Covid-19 patients is 9 times that of influenza patients. And this also may be related to the slower development of COVID-19 than other viral pneumonias (19). It is worth noting that tree-in-bud was observed in 27.66% of influenza pneumonia cases, and similar results were observed by Shiley *et al.* (21), but almost no tree-in-bud was observed in COVID-19. Compared with other viral pneumonias, CMV pneumonia often presents as a characteristic bronchiectasis, and immunocompromise is an important risk factor. In previous studies, it has been called "AIDS associated bronchiectasis" (22). With this information combined with the clinical data, radiologists can better identify the type of viral pneumonia (23). Currently, Duan *et al.* and Gu *et al.* observe the CT findings of COVID-19 patients in different populations, such as children, adults, and the elderly (24,25). They found that compared with adults, pediatric COVID-19 patients are characterized by lower incidence, milder clinical symptoms, shorter course of disease, and fewer severe cases. In the elderly, lung lesions are more likely to progress. Study has shown that age is an independent wind direction factor for COVID-19 (26). In-hospital mortality increases linearly with age, with the highest mortality in patients over 80 years of age.

This study has some limitations. First, although we tried our best to collect the clinical and imaging data of patients with viral pneumonia in Yunnan Province, the numbers of confirmed cases of adenovirus, measles virus, herpes virus and other viruses were relatively small, but the differences in imaging signs among them are very interesting and will be studied in the future. Second, most of the included CMV pneumonia patients had AIDS, which is likely to cause a selection bias regarding other CMV pneumonia patients. Third, different populations, such as infants, children and elderly adults, may be susceptible to different viruses, and their signs of pulmonary lesions on imaging might be different. Because of the sample size, we did not perform a subgroup analysis for age. In future studies, more effort should be made to determine the differences in the imaging characteristics of different populations.

In summary, the analysis and comparison of the chest CT findings of COVID-19 and other viral pneumonias showed that the chest CT findings partially overlapped, but many significant imaging features could still be observed, which

is helpful for the early differential diagnosis of COVID-19 and the development of more accurate clinical diagnosis and treatment strategies.

Acknowledgments

The authors express their appreciation for all the hospital staff for their efforts to combat the COVID-19 outbreak. Thank you to all the patients who participated in this study.
Funding: None.

Footnote

Reporting Checklist: The authors have completed the STROBE reporting checklist. Available at http://dx.doi.org/10.21037/apm-20-2479

Data Sharing Statement: Available at http://dx.doi.org/10.21037/apm-20-2479

Conflicts of Interest: All authors have completed the ICMJE uniform disclosure form (available at http://dx.doi.org/10.21037/apm-20-2479). The authors have no conflicts of interest to declare.

Ethical Statement: The authors are accountable for all aspects of the work in ensuring that questions related to the accuracy or integrity of any part of the work are appropriately investigated and resolved. The study was conducted in accordance with the Declaration of Helsinki (as revised in 2013). The retrospective study was approved by the institutional committee of the First Affiliated Hospital of Kunming Medical University. Informed consent was waived because the study was retrospective in design.

References

1. Zhu N, Zhang D, Wang W, et al. A Novel Coronavirus from Patients with Pneumonia in China, 2019. N Engl J Med 2020;382:727-33.
2. Guan WJ, Ni ZY, Hu Y, et al. Clinical Characteristics of Coronavirus Disease 2019 in China. N Engl J Med 2020;382:1708-20.
3. Qiu H, Wu J, Hong L, et al. Clinical and epidemiological features of 36 children with coronavirus disease 2019 (COVID-19) in Zhejiang, China: an observational cohort study. Lancet Infect Dis 2020;20:689-96.
4. Chen N, Zhou M, Dong X, et al. Epidemiological and clinical characteristics of 99 cases of 2019 novel coronavirus pneumonia in Wuhan, China: a descriptive study. Lancet 2020;395:507-13.
5. Fowlkes A, Steffens A, Temte J, et al. Incidence of medically attended influenza during pandemic and postpandemic seasons through the Influenza Incidence Surveillance Project, 2009-13. Lancet Respir Med 2015;3:709-18.
6. Moriyama M, Hugentobler WJ, Iwasaki A. Seasonality of Respiratory Viral Infections. Annu Rev Virol 2020;7:83-101.
7. Li Y, Reeves RM, Wang X, et al. Global patterns in monthly activity of influenza virus, respiratory syncytial virus, parainfluenza virus, and metapneumovirus: a systematic analysis. Lancet Glob Health 2019;7:e1031-e1045.
8. Fang Y, Zhang H, Xie J, et al. Sensitivity of Chest CT for COVID-19: Comparison to RT-PCR. Radiology 2020;296:E115-E117.
9. Koo HJ, Lim S, Choe J, et al. Radiographic and CT Features of Viral Pneumonia. Radiographics 2018;38:719-39.
10. Miller WT Jr, Mickus TJ, Barbosa E Jr, et al. CT of viral lower respiratory tract infections in adults: comparison among viral organisms and between viral and bacterial infections. AJR Am J Roentgenol 2011;197:1088-95.
11. Ai T, Yang Z, Hou H, et al. Correlation of Chest CT and RT-PCR Testing in Coronavirus Disease 2019 (COVID-19) in China: A Report of 1014 Cases. Radiology 2020;296:E32-E40.
12. Chung M, Bernheim A, Mei X, et al. CT Imaging Features of 2019 Novel Coronavirus (2019-nCoV). Radiology 2020;295:202-7.
13. Caruso D, Zerunian M, Polici M, et al. Chest CT Features of COVID-19 in Rome, Italy. Radiology 2020;296:E79-E85.
14. Pan F, Ye T, Sun P, et al. Time Course of Lung Changes On Chest CT During Recovery From 2019 Novel Coronavirus (COVID-19) Pneumonia. Radiology 2020;295:715-21.

15. Pan Y, Guan H, Zhou S, et al. Initial CT findings and temporal changes in patients with the novel coronavirus pneumonia (2019-nCoV): a study of 63 patients in Wuhan, China. Eur Radiol 2020;30:3306-9.
16. China National Health Commission. Diagnosis and treatment of pneumonitis caused by new coronavirus (trial version 6). Available online: http://www.nhe.gov.en/yzygj/s7653p/202002/8334a8326dd94d329df351d7da8aefe2.shtml. Accessed February 19, 2020.
17. Shi H, Han X, Jiang N, et al. Radiological findings from 81 patients with COVID-19 pneumonia in Wuhan, China: a descriptive study. Lancet Infect Dis 2020;20:425-34.
18. Zhao D, Yao F, Wang L, et al. A comparative study on the clinical features of COVID-19 pneumonia to other pneumonias. Clin Infect Dis 2020;71:756-61.
19. Tang X, Du R, Wang R, et al. Comparison of hospitalized patients with ARDS caused by COVID-19 and H1N1. Chest 2020;158:195-205.
20. Ackermann M, Verleden SE, Kuehnel M, et al. Pulmonary Vascular Endothelialitis, Thrombosis, and Angiogenesis in Covid-19. N Engl J Med 2020;383:120-8.
21. Shiley KT, Van Deerlin VM, Miller WT Jr. Chest CT features of community-acquired respiratory viral infections in adult inpatients with lower respiratory tract infections. J Thorac Imaging 2010;25:68-75.
22. McGuinness G, Naidich DP, Garay S, et al. AIDS associated bronchiectasis: CT features. J Comput Assist Tomogr 1993;17:260-6.
23. Bai HX, Hsieh B, Xiong Z, et al. Performance of radiologists in differentiating COVID-19 from viral pneumonia on chest CT. Radiology 2020;296:E46-E54.
24. Duan YN, Zhu YQ, Tang LL, et al. CT features of novel coronavirus pneumonia (COVID-19) in children. Eur Radiol 2020;30:4427-33.
25. Gu Q, Ouyang X, Xie A, et al. A retrospective study of the initial chest CT imaging findings in 50 COVID-19 patients stratified by gender and age. J Xray Sci Technol 2020;28:875-84.
26. Rosenthal N, Cao Z, Gundrum J, et al. Risk Factors Associated With In-Hospital Mortality in a US National Sample of Patients With COVID-19. JAMA Netw Open 2020;3:e2029058.

(English Language Editor: A. Kassem)

Cite this article as: Huang Y, Jiang Y, Li Z, Han D, Wu L, Ma J, Wang P, Xie Y, Li Z, Li X, Hong M, Zhou J, Duan C, Yang Y, Zhao W, Yuan F, Wang K, Yi W, He B. Comparison of initial high-resolution computed tomography (HRCT) features of coronavirus disease 2019 (COVID-19) pneumonia and other viral pneumonias. Ann Palliat Med 2021;10(1):560-571. doi: 10.21037/apm-20-2479

